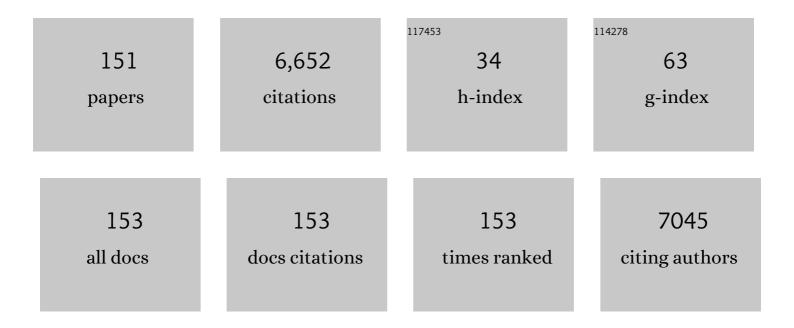
List of Publications by Year in descending order

Source: https://exaly.com/author-pdf/9778289/publications.pdf Version: 2024-02-01



#	Article	IF	CITATIONS
1	Scanning Electron Microscopy and X-ray Microanalysis. , 2003, , .		1,309
2	Scanning Electron Microscopy and X-Ray Microanalysis. , 2018, , .		955
3	TEM Sample Preparation and FIB-Induced Damage. MRS Bulletin, 2007, 32, 400-407.	1.7	723
4	Automated Analysis of SEM X-Ray Spectral Images: A Powerful New Microanalysis Tool. Microscopy and Microanalysis, 2003, 9, 1-17.	0.2	297
5	Solidification of Nb-bearing superalloys: Part I. Reaction sequences. Metallurgical and Materials Transactions A: Physical Metallurgy and Materials Science, 1998, 29, 2785-2796.	1.1	153
6	Lithographically Defined Three-Dimensional Graphene Structures. ACS Nano, 2012, 6, 3573-3579.	7.3	152
7	Crystallography of YBa ₂ Cu ₃ O _{6+<i>x</i>} thin film-substrate interfaces. Journal of Materials Research, 1989, 4, 1072-1081.	1.2	147
8	Carbonitride precipitation in niobium/vanadium microalloyed steels. Metallurgical and Materials Transactions A - Physical Metallurgy and Materials Science, 1987, 18, 211-222.	1.4	117
9	Microstructural evolution of Pb(Zr, Ti)O ₃ thin films prepared by hybrid metallo-organic decomposition. Journal of Materials Research, 1992, 7, 1876-1882.	1.2	116
10	Room-Temperature Voltage Tunable Phonon Thermal Conductivity via Reconfigurable Interfaces in Ferroelectric Thin Films. Nano Letters, 2015, 15, 1791-1795.	4.5	116
11	Microstructural and mechanical properties investigation of electrodeposited and annealed LIGA nickel structures. Metallurgical and Materials Transactions A: Physical Metallurgy and Materials Science, 2002, 33, 539-554.	1.1	103
12	The effect of boron on the chemistry of grain boundaries in stoichiometric Ni ₃ Al. The Philosophical Magazine: Physics of Condensed Matter B, Statistical Mechanics, Electronic, Optical and Magnetic Properties, 1988, 57, 379-385.	0.6	92
13	Phase identification in a scanning electron microscope using backscattered electron Kikuchi patterns. Journal of Research of the National Institute of Standards and Technology, 1996, 101, 301.	0.4	85
14	Tomographic Spectral Imaging with Multivariate Statistical Analysis: Comprehensive 3D Microanalysis. Microscopy and Microanalysis, 2006, 12, 36-48.	0.2	79
15	A consistent definition of probe size and spatial resolution in the analytical electron microscope. Journal of Microscopy, 1987, 147, 289-303.	0.8	78
16	Group IVA irons: New constraints on the crystallization and cooling history of an asteroidal core with a complex history. Geochimica Et Cosmochimica Acta, 2011, 75, 6821-6843.	1.6	76
17	The formation of plessite in meteoritic metal. Meteoritics and Planetary Science, 2006, 41, 553-570.	0.7	75
18	Linking microstructural evolution and macro-scale friction behavior in metals. Journal of Materials Science, 2017, 52, 2780-2799.	1.7	75

#	Article	IF	CITATIONS
19	Single Crystals of Pb(Mg _{1/3} Nb _{2/3})O ₃ —35 mol% PbTiO ₃ from Polycrystalline Precursors. Journal of the American Ceramic Society, 1998, 81, 244-248.	1.9	73
20	An analytical electron microscope study of the kinetics. Metallurgical and Materials Transactions A - Physical Metallurgy and Materials Science, 1984, 15, 99-105.	1.4	60
21	Fatigue of metallic microdevices and the role of fatigue-induced surface oxides. Acta Materialia, 2004, 52, 1609-1619.	3.8	57
22	Characterization of the Fe-Co-1.5V soft ferromagnetic alloy processed by Laser Engineered Net Shaping (LENS). Additive Manufacturing, 2018, 21, 41-52.	1.7	56
23	The measurement and calculation of the Xâ€ray spatial resolution obtained in the analytical electron microscope. Journal of Microscopy, 1990, 160, 41-53.	0.8	52
24	Use of reciprocal lattice layer spacing in electron backscatter diffraction pattern analysis. Ultramicroscopy, 2000, 81, 67-81.	0.8	50
25	The role of substrate plasticity on the tribological behavior of diamond-like nanocomposite coatings. Acta Materialia, 2008, 56, 1956-1966.	3.8	50
26	Achieving high strength and ductility in traditionally brittle soft magnetic intermetallics via additive manufacturing. Acta Materialia, 2019, 180, 149-157.	3.8	47
27	Investigating active slip planes in tantalum under compressive load: Crystal plasticity and slip trace analyses of single crystals. Acta Materialia, 2020, 185, 1-12.	3.8	47
28	The effects of both deviation from stoichiometry and boron on grain boundaries in Ni ₃ Al. The Philosophical Magazine: Physics of Condensed Matter B, Statistical Mechanics, Electronic, Optical and Magnetic Properties, 1990, 62, 659-676.	0.6	45
29	Three dimensional nickel–graphene core–shell electrodes. Journal of Materials Chemistry, 2012, 22, 23749.	6.7	45
30	Definition of the spatial resolution of X-ray microanalysis in thin foils. Ultramicroscopy, 1992, 47, 121-132.	0.8	44
31	Focused Ion Beam Induced Microstructural Alterations: Texture Development, Grain Growth, and Intermetallic Formation. Microscopy and Microanalysis, 2011, 17, 386-397.	0.2	43
32	Thermal history and origin of the IVB iron meteorites and their parent body. Geochimica Et Cosmochimica Acta, 2010, 74, 4493-4506.	1.6	42
33	Mechanical and Corrosion Properties of Additively Manufactured CoCrFeMnNi High Entropy Alloy. Additive Manufacturing, 2019, 29, 100833.	1.7	42
34	Initiation and growth of the grain boundary discontinuous precipitation reaction. Acta Metallurgica, 1981, 29, 1343-1355.	2.1	41
35	Controlled fabrication of nanopores using a direct focused ion beam approach with back face particle detection. Nanotechnology, 2008, 19, 235304.	1.3	41
36	Thermal histories of IVA iron meteorites from transmission electron microscopy of the cloudy zone microstructure. Meteoritics and Planetary Science, 2009, 44, 343-358.	0.7	35

#	Article	IF	CITATIONS
37	Thermal and collisional history of Tishomingo iron meteorite: More evidence for early disruption of differentiated planetesimals. Geochimica Et Cosmochimica Acta, 2014, 124, 34-53.	1.6	32
38	Thermal and impact histories of reheated group IVA, IVB, and ungrouped iron meteorites and their parent asteroids. Meteoritics and Planetary Science, 2011, 46, 1227-1252.	0.7	31
39	Phase identification of individual crystalline particles by electron backscatter diffraction. Journal of Microscopy, 2001, 201, 59-69.	0.8	30
40	Comparison of Channeling Contrast between Ion and Electron Images. Microscopy and Microanalysis, 2013, 19, 344-349.	0.2	30
41	Morphology and Growth Kinetics of Straight and Kinked Tin Whiskers. Metallurgical and Materials Transactions A: Physical Metallurgy and Materials Science, 2013, 44, 1485-1496.	1.1	27
42	Improving the quality of electron backscatter diffraction (EBSD) patterns from nanoparticles. Journal of Microscopy, 2002, 206, 170-178.	0.8	26
43	Forensic analysis of bioagents by X-ray and TOF-SIMS hyperspectral imaging. Forensic Science International, 2008, 179, 98-106.	1.3	26
44	Development of Gd-Enriched Alloys for Spent Nuclear Fuel Applications - Part 1: Preliminary Characterization of Small Scale Gd-Enriched Stainless Steels. Journal of Materials Engineering and Performance, 2003, 12, 206-214.	1.2	25
45	On-chip laboratory suite for testing of free-standing metal film mechanical properties, Part II – Experiments. Acta Materialia, 2008, 56, 3313-3326.	3.8	25
46	Characterization of pore morphology in molecular crystal explosives by focused ion-beam nanotomography. Journal of Materials Research, 2010, 25, 1362-1370.	1.2	25
47	Microstructure and 90° domain assemblages of Pb(Zr, Ti)O ₃ //RuO ₂ capacitors as a function of Zr-to-Ti stoichiometry. Journal of Materials Research, 1996, 11, 2309-2317.	1.2	23
48	Comparison of ferroelectric domain assemblages in Pb(Zr,Ti)O3thin films and bulk ceramics. Ferroelectrics, 1999, 221, 209-218.	0.3	23
49	An Investigation of the Massive Transformation from Ferrite to Austenite in Laser-Welded Mo-Bearing Stainless Steels. Metallurgical and Materials Transactions A: Physical Metallurgy and Materials Science, 2011, 42, 700-716.	1.1	23
50	The hardness and strength of metal tribofilms: An apparent contradiction between nanoindentation and pillar compression. Acta Materialia, 2012, 60, 1712-1720.	3.8	23
51	Effects of current density on the structure of Ni and Ni–Mn electrodeposits. Journal of Applied Electrochemistry, 2006, 36, 669-676.	1.5	22
52	The Effects of Pre-Oxidation and Alloy Chemistry of Austenitic Stainless Steels on Glass/Metal Sealing. Oxidation of Metals, 2010, 73, 311-335.	1.0	22
53	Wear resistant electrically conductive Au–ZnO nanocomposite coatings synthesized by e-beam evaporation. Wear, 2013, 302, 955-962.	1.5	22
54	Application of Electron Backscatter Diffraction Techniques to Quenched and Partitioned Steels. Microscopy and Microanalysis, 2011, 17, 368-373.	0.2	21

#	Article	IF	CITATIONS
55	Multivariate statistical approach to electron backscattered diffraction. Ultramicroscopy, 2008, 108, 567-578.	0.8	20
56	Surface alloy depletion and martensite formation during glass to metal joining of austenitic stainless steels. Science and Technology of Welding and Joining, 2012, 17, 321-332.	1.5	20
57	A Study of Selective Etching of Carbides in Steel. Microscopy and Microanalysis, 2004, 10, 76-77.	0.2	19
58	Microstructure and thermal history of metal particles in CH chondrites. Meteoritics and Planetary Science, 2007, 42, 913-933.	0.7	19
59	Controlling the extent of atomic ordering in intermetallic alloys through additive manufacturing. Additive Manufacturing, 2019, 28, 772-780.	1.7	19
60	Phase Identification Using Electron Backscatter Diffraction in the Scanning Electron Microscope. , 2000, , 75-89.		18
61	Experimental determination of lightâ€element <i>k</i> â€factors using the extrapolation technique: Oxygen segregation in aluminium nitride. Journal of Microscopy, 1992, 167, 287-302.	0.8	17
62	Solidification and welding metallurgy of Thermo-Span alloy. Science and Technology of Welding and Joining, 1997, 2, 220-230.	1.5	17
63	Structural Variants in Attempted Heteroepitaxial Growth of B12As2 on 6H–SiC (0001). Journal of Materials Research, 2005, 20, 3004-3010.	1.2	17
64	Electrodeposition of Ni from Low-Temperature Sulfamate Electrolytes. Journal of the Electrochemical Society, 2006, 153, C325.	1.3	17
65	Residual thermal stresses in MoSi2–Mo5Si3 in-situ composites. Materials Science & Engineering A: Structural Materials: Properties, Microstructure and Processing, 1999, 261, 261-269.	2.6	16
66	Using the FIB to characterize nanoparticle materials. Journal of Microscopy, 2004, 214, 222-236.	0.8	16
67	Effects of Low Temperature on Hydrogen-Assisted Crack Growth in Forged 304L Austenitic Stainless Steel. Metallurgical and Materials Transactions A: Physical Metallurgy and Materials Science, 2016, 47, 4334-4350.	1.1	16
68	Gallium Phase Formation in Cu During 30kV Ga+ FIB Milling. Microscopy and Microanalysis, 2006, 12, 1248-1249.	0.2	15
69	Selective Growth of CdTe on Nano-patterned CdS via Close-Space Sublimation. Journal of Electronic Materials, 2014, 43, 2651-2657.	1.0	15
70	Domain imaging in ferroelectric thin films via channeling-contrast backscattered electron microscopy. Journal of Materials Science, 2017, 52, 1071-1081.	1.7	15
71	Electrical contact uniformity and surface oxidation of ternary chalcogenide alloys. AIP Advances, 2019, 9, 015125.	0.6	15
72	Oxide dispersion strengthening of nickel electrodeposits for microsystem applications. Metallurgical and Materials Transactions A: Physical Metallurgy and Materials Science, 2004, 35, 2351-2360.	1.1	14

#	Article	IF	CITATIONS
73	EBSD of Ceramic Materials. , 2000, , 299-318.		13
74	<title>Effect of Cu at Al grain boundaries on electromigration behavior in Al thin films</title> . , 1991, , .		11
75	High resolution at low beam energy in the SEM: resolution measurement of a monochromated SEM. Scanning, 2011, 33, 147-154.	0.7	11
76	Grain Boundary Chemistry in Al-Cu Metallizations as Determined by Analytical Electron Microscopy. Materials Research Society Symposia Proceedings, 1991, 229, 303.	0.1	10
77	The Effect of Cu Alloying on Al Alloy Thin Films: Microstructural Mechanisms That Enhance Electromigration Resistance. Materials Research Society Symposia Proceedings, 1993, 309, 359.	0.1	10
78	SEM Analysis of Oxide Thin Films and Reactions. Journal of the American Ceramic Society, 1999, 82, 1644-1646.	1.9	9
79	Three-Dimensional (3D) Reconstruction of AlFeSi Intermetallic Particles in 6xxx Aluminum Alloys Using the Focused Ion Beam (FIB). Microscopy and Microanalysis, 2004, 10, 1138-1139.	0.2	9
80	Application of Diamond-Like Nanocomposite Tribological Coatings on LIGA Microsystem Parts. Journal of Microelectromechanical Systems, 2009, 18, 695-704.	1.7	9
81	Electrical resistivity of Au-ZnO nanocomposite films. Journal of Applied Physics, 2013, 113, .	1.1	9
82	Rethinking scaling laws in the high-cycle fatigue response of nanostructured and coarse-grained metals. International Journal of Fatigue, 2020, 134, 105472.	2.8	9
83	Analysis of the reaction between 60Sn-40Pb solder with a Pd-Pt-Ag-Cu-Au alloy. Journal of Electronic Materials, 1993, 22, 185-194.	1.0	8
84	Iron oxide on (001) MgO. Philosophical Magazine A: Physics of Condensed Matter, Structure, Defects and Mechanical Properties, 1999, 79, 2887-2898.	0.8	8
85	Screen Printing to Achieve Highly Textured Bi ₄ Ti ₃ O ₁₂ . Journal of the American Ceramic Society, 2010, 93, 1922-1926.	1.9	8
86	Parallel simulation of electron-solid interactions for electron microscopy modeling. Journal of Supercomputing, 1992, 6, 139-151.	2.4	7
87	Preferred heteroepitaxial orientations of ZnO nanorods on Ag. Journal of Materials Research, 2010, 25, 1352-1361.	1.2	7
88	On the thermal stability of physical vapor deposited oxide-hardened nanocrystalline gold thin films. Journal of Applied Physics, 2015, 117, .	1.1	7
89	Equal channel angular extrusion for bulk processing of Fe–Co–2V soft magnetic alloys, part II: Texture analysis and magnetic properties. Journal of Materials Research, 2018, 33, 2176-2188.	1.2	7
90	Role of defects on the surface properties of HfC. Applied Surface Science, 2019, 495, 143500.	3.1	7

#	Article	IF	CITATIONS
91	Ex Situ Photoelectron Emission Microscopy of Polycrystalline Bismuth and Antimony Telluride Surfaces Exposed to Ambient Oxidation. ACS Applied Materials & Interfaces, 2021, 13, 18218-18226.	4.0	6
92	Scanning ultrafast electron microscopy reveals photovoltage dynamics at a deeply buried <mml:math xmlns:mml="http://www.w3.org/1998/Math/MathML"><mml:mrow><mml:mi>p</mml:mi><mml:mtext>â^'mathvariant="normal">O<mml:mn>2</mml:mn></mml:mtext></mml:mrow> interface. Physical Review B, 2021, 104, .</mml:math 	ıml:mtext> 1.1	<mml:mi>Si<!--</td--></mml:mi>
93	Solder flow on narrow copper strips. Journal of Electronic Materials, 1996, 25, 1099-1107.	1.0	5
94	Tomographic Spectral Imaging: Comprehensive 3D X-ray Microanalysis. Microscopy and Microanalysis, 2003, 9, 1004-1005.	0.2	5
95	Tomographic Spectral Imaging with a Dual-Beam FIB/SEM: 3D Microanalysis. Microscopy and Microanalysis, 2004, 10, 1132-1133.	0.2	5
96	Characterization of the mechanical behavior of wear surfaces on single crystal nickel by nanomechanical techniques. Journal of Materials Research, 2009, 24, 844-852.	1.2	5
97	Solidification and welding metallurgy of Thermo-Span alloy. Science and Technology of Welding and Joining, 1997, 2, 220-230.	1.5	5
98	Analytical electron microscopy of internally oxidized low Si-Al steel. Metallurgical and Materials Transactions A - Physical Metallurgy and Materials Science, 1988, 19, 953-959.	1.4	4
99	Progress in the Design of an Improved High-Temperature 1 Percent CrMoV Rotor Steel. Journal of Engineering Materials and Technology, Transactions of the ASME, 1990, 112, 99-115.	0.8	4
100	Electron Backscatter Diffraction in the SEM: A Tutorial. Microscopy and Microanalysis, 2002, 8, 724-725.	0.2	4
101	Evaluating SEM performance from the contrast transfer function. , 2010, , .		4
102	Nanopatterning and bandgap grading to reduce defects in CdTe solar cells. , 2012, , .		4
103	Application of Electron Backscatter Diffraction for Crystallographic Characterization of Tin Whiskers. Microscopy and Microanalysis, 2012, 18, 876-884.	0.2	4
104	Modeling ion-solid interactions for imaging applications. MRS Bulletin, 2014, 39, 342-346.	1.7	4
105	Focused Ion Beam Preparation of Low Melting Point Metals: Lessons Learned From Indium. Microscopy and Microanalysis, 2022, 28, 603-610.	0.2	4
106	Austenite recrystallization in. Metallurgical and Materials Transactions A - Physical Metallurgy and Materials Science, 1987, 18, 481-483.	1.4	3
107	Electron Backscatter Diffraction In The Sem: Is Electron Diffraction In The Tem Obsolete?. Microscopy and Microanalysis, 1997, 3, 879-880.	0.2	3
108	On the Influence of Applied Fields on Spinel Formation. Materials Research Society Symposia Proceedings, 1999, 586, 151.	0.1	3

#	Article	IF	CITATIONS
109	Application of FIB and TEM for the Characterization of Dewetting Behavior on Ceramics. Microscopy and Microanalysis, 2002, 8, 562-563.	0.2	3
110	Specimen Preparation of Hard Materials: Metals, Ceramics, Rocks, Minerals, Microelectronic and Packaged Devices, Particles, and Fibers. , 2003, , 537-564.		3
111	Microscopy and Microanalysis of Nano-Scale Materials. Microscopy Today, 2006, 14, 6-15.	0.2	3
112	Characterization of Continuous and Discontinuous Precipitation Phases in Pd-Rich Precious Metal Alloys. Metallurgical and Materials Transactions A: Physical Metallurgy and Materials Science, 2014, 45, 3755-3766.	1.1	3
113	Comparison of Orientation Mapping in SEM and TEM. Microscopy and Microanalysis, 2020, 26, 630-640.	0.2	3
114	The Effects of Annealing After Equal Channel Angular Extrusion (ECAE) on Mechanical and Magnetic Properties of 49Fe-49Co-2V Alloy. Metallurgical and Materials Transactions A: Physical Metallurgy and Materials Science, 2021, 52, 4090-4099.	1.1	3
115	Mechanism of FIB-Induced Phase Transformation in Austenitic Steel. Microscopy and Microanalysis, 2022, 28, 70-82.	0.2	3
116	Characterization of Nanoparticle Films and Structures Using Focused Ion Beam Milling and Transmission Electron Microscopy. Microscopy and Microanalysis, 2002, 8, 1144-1145.	0.2	2
117	The Effects of 304L Stainless Steel Pre-Oxidation on Bonding to Alkali Barium Silicate Glass. Ceramic Engineering and Science Proceedings, 0, , 145-157.	0.1	2
118	Microdiffraction phase identification in the scanning electron microscope (SEM). Powder Diffraction, 2004, 19, 100-103.	0.4	1
119	On the Evolution of Friction-Induced Nanostructures in Single Crystal Nickel. , 2005, , 317.		1
120	Electron Beam-Based Methods for Bioforensic Investigations. , 2011, , 421-729.		1
121	Method for electrical-structural correlation in isolated CdTe/CdS islands. , 2014, , .		1
122	Nanoscale photovoltaic performance in micro/nanopatterned CdTe-CdS thin film solar cells. , 2014, , .		1
123	Characterization of Void-Dominated Ductile Failure in Pure Ta. Microscopy and Microanalysis, 2015, 21, 1163-1164.	0.2	1
124	Compositional Mapping. , 2018, , 413-439.		1
125	Energy Dispersive X-Ray Spectrometry in Ultra-high Vacuum Environments. , 1995, , 83-99.		1
126	Crystallographic phase identification in the SEM: Backscattered electron kikuchi patterns. Proceedings Annual Meeting Electron Microscopy Society of America, 1993, 51, 772-773.	0.0	1

#	Article	IF	CITATIONS
127	Carbonitride precipitation in niobium/vanadium microalloyed steels. Metallurgical and Materials Transactions A - Physical Metallurgy and Materials Science, 1987, 18, 211-222.	1.4	1
128	Analytical electron microscopy of internally oxidized mn-p steel. Metallurgical and Materials Transactions A - Physical Metallurgy and Materials Science, 1988, 19, 1876-1878.	1.4	0
129	AEM in Steel Research. Jom, 1988, 40, 8-12.	0.9	0
130	Energy Dispersive Spectrometry in the AEM. Microscopy and Microanalysis, 1998, 4, 186-187.	0.2	0
131	Spectral Imaging and Automated Multivariate Statistical Analysis of the Ourique Meteorite. Microscopy and Microanalysis, 2004, 10, 892-893.	0.2	Ο
132	FIB Preparation of Samples for EBSD: Applications to Wear Studies of MEMS Materials. Microscopy and Microanalysis, 2004, 10, 1130-1131.	0.2	0
133	Characterization of Nano-Crystalline Materials Using Electron Backscatter Diffraction in the Scanning Electron Microscope. , 2005, , 401-425.		Ο
134	Mineral Analyses of Extraterrestrial Metal. Microscopy and Microanalysis, 2014, 20, 1674-1675.	0.2	0
135	Microscopy & Microanalysis 2016. Microscopy Today, 2016, 24, 52-55.	0.2	Ο
136	Microscopy & Microanalysis 2016 in Columbus, Ohio. Microscopy Today, 2016, 24, 38-41.	0.2	0
137	Measuring Carbon in Steel Using Calibration Curves on the Microprobe; Failed Cap Screw Study. Microscopy and Microanalysis, 2017, 23, 516-517.	0.2	Ο
138	Challenges Associated with Transmission Experiments in the SEM. Microscopy and Microanalysis, 2017, 23, 556-557.	0.2	0
139	Characterizing Crystalline Materials in the SEM. , 2018, , 491-515.		0
140	Focused Ion Beam Applications in the SEM Laboratory. , 2018, , 517-528.		0
141	Electron Microscopy and Microanalysis for Wear Surface Characterization. Microtechnology and MEMS, 2018, , 3-28.	0.2	0
142	Preparation of samples: Why use Ga, Xe or photons?. Microscopy and Microanalysis, 2021, 27, 16-17.	0.2	0
143	Microstructure and Reliability of Surface Micromachined Polysilicon Used for MEMS. , 2003, , .		0
144	The spatial resolution of x-ray microanalysis in thin foils. Proceedings Annual Meeting Electron Microscopy Society of America, 1991, 49, 472-473.	0.0	0

#	Article	IF	CITATIONS
145	High-spatial-resolution microanalysis in the analytical electron microscope: a tutorial. Proceedings Annual Meeting Electron Microscopy Society of America, 1992, 50, 1122-1123.	0.0	Ο
146	High-spatial-resolution x-ray microanalysis: Comparison of experiment and incoherent scattering calculations. Proceedings Annual Meeting Electron Microscopy Society of America, 1993, 51, 590-591.	0.0	0
147	Massively parallel Monte Carlo simulations of images and analytical data for Electron Microscopy. Proceedings Annual Meeting Electron Microscopy Society of America, 1994, 52, 910-911.	0.0	0
148	High spatial resolution x-ray microanalysis of interfaces. Proceedings Annual Meeting Electron Microscopy Society of America, 1995, 53, 284-285.	0.0	0
149	The effects of probe characteristics and specimen thickness on the spatial resolution in the AEM. Proceedings Annual Meeting Electron Microscopy Society of America, 1989, 47, 202-203.	0.0	0
150	High-resolution x-ray elemental images. Proceedings Annual Meeting Electron Microscopy Society of America, 1989, 47, 204-205.	0.0	0
151	Atomic step disorder on polycrystalline surfaces leads to spatially inhomogeneous work functions. Journal of Vacuum Science and Technology A: Vacuum, Surfaces and Films, 2022, 40, 023207.	0.9	О